Theoretical Studies of Ribose and Its Radicals Produced by Hydrogen Abstraction from Ring Carbons

Ning Luo, Arkadi Litvin, and Roman Osman*

Department of Physiology and Biophysics, Mount Sinai School of Medicine of the City University of New York, One Gustave L. Levy Place, New York, New York 10029

Received: June 29, 1998

The energies and structures of ribose and its radicals produced by hydrogen abstraction from each of the four ribose ring carbons were studied by ab initio quantum chemical methods including geometry optimization at the HF/6-31G level. Two types of the sugar ring pseudorotational states (N-type and S-type) and different orientations of the hydroxyl groups on C_2 and C_3 were identified. Three energy minima are found for the N-type conformation of ribose with different orientations of the two hydroxy groups while only two energy minima are found for the S-type conformation. The N-type pseudorotamer is more stable than the S-type. The radicals formed by H abstraction from the carbons of ribose all show two forms that can be classified as N-type and S-type conformers. The ring of the radicals is flattened compared to that of ribose, with the C_2 radical showing the most significant reduction in puckering amplitude. The possibility of radical inversion adds additional complexity to the conformational properties of ribose radicals. In the C_1 and C_4 radicals, the inverted orientations are minima more stable than the original ones. The bond dissociation energies of the various hydrogens lie in a range of 87−93 kcal/mol and, in distinction from deoxyribose, they are all of comparable strength.

Introduction

Deoxyribose and ribose radicals generated by hydrogen abstraction are important intermediates in radiation damage of DNA and RNA.[1] Many experimental studies on radiation damage to the sugars of both DNA and RNA have been carried out demonstrating that radiation damage of RNA is distinctly different from that of DNA. It is clear that an initial damage to the base in RNA can be effectively transferred to the sugar but such a mechanism is much less likely in DNA. It was demonstrated that such a transfer occurs through H_2 abstraction by the base radical and the increased susceptibility of H_2 abstraction in ribose compared to that in deoxyribose was attributed to the presence of the 2-OH group.[2−4] In our previous work it was shown that the susceptibility of H abstraction should be reflected in the bond dissociation energy (BDE) [5] but the strengths of the various C−H bonds in ribose has not been determined experimentally. In an attempt to estimate the BDE in ribose we realized that a thorough study of the conformational properties of ribose and its radicals is necessary. Only a few theoretical works have performed a conformational analysis of ribose,[6,7] and as far as we know no theoretical studies of the ribose radicals are known. Experimental work on ribose radicals has been limited to the identification of the localization of the radical site but no structural inferences have been made.[8,9]

The differences between DNA and RNA behavior in radiation damage processes induced by hydrogen abstraction stem from the different conformational properties of the deoxyribose versus the ribose sugar. It is well-known that the overall conformations of DNA and RNA are different due to the presence of 2′-OH group on ribose. Experimental data show that, similar to deoxyribose, the conformation of ribose in various type of RNA's and oligonucleotides are clustered around two particular conformations. One cluster is the 3′-*endo* (N-type) conformation located in the northern part of the polar map of the puckering amplitude and pseudorotational phase angle, and the other is the 2′-*endo* (S-type) conformation located on the southern part of the map.[10−17] These pseudorotational energy minima have been also confirmed by theoretical calculations.[7,6] However, while deoxyribose is predominantly in the S-type conformation, leading to a B-DNA conformation, the ribose in RNA is predominantly N-type,[10] producing an A-RNA structure. Such a conformational difference leads to different accessibility of sugar hydrogens for abstraction by hydroxyl or base radicals. Also, the presence of a 2′-OH group on ribose in RNA should affect the susceptibility of H_2' abstraction, presumably by lowering the C_2'−H bond strength.

A previous theoretical study of deoxyribose radicals produced by hydrogen abstraction of both N-and S-type deoxyribose[5] revealed that the structures of the radicals are significantly different from those of deoxyribose. The puckering of the radicals was reduced, indicating a ring flattening. The pseudorotational phase angles were shifted in a regular pattern with changes ranging up to 60°. Most importantly, the hydrogen abstraction from C_2 was the least energetically favorable because the C_2−H bond strength was distinctly larger than all the other bonds. This conclusion was confirmed by a recent study.[18] It is therefore interesting to examine how the 2-OH group in ribose affects the hydrogen abstraction from C_2 as well as the conformational properties of the ribose ring upon radical formation.

We report here the minimum energy conformations of (*R*)-2-amino-(*S*)-3-hydroxy-(*S*)-4-hydroxy-(*S*)-5-methyltetrahydrofuran (5-deoxy-β-D-erythro-pentafuranosylamine) as a simplified model of a ribonucleoside. Thus, the CH_2OH group in the 5-position was replaced with a methyl and the base connected to C_1 with an amine group, NH_2. We also report the energies and structures of the radicals produced by H abstraction from

10.1021/jp982799v CCC: $18.00
Published on Web 01/20/1999

each of the four ring carbons in the ribose model. These provide estimates for the enthalpies of H abstraction and the bond strengths of each hydrogen. Finally, we compare these results with deoxyribose and its radicals.[5] A better understanding of the process of RNA radiation damage, in addition to its own biological and biochemical significance, should serve as an important comparison to the corresponding process in DNA and will enhance our understanding of the mechanisms governing these processes.

Method

All calculations were performed with Gaussian 94.[19] Geometries of each structure were fully optimized at HF/6-31G level. Zero-point energies (ZPE) at HF/6-31G and single-point energy of HF/6-31G*, MP2/6-31G*, BLYP/6-31G*, and Becke's half-and-half density functional with 6-31G(d,p) basis set (BH/6-31G(d,p)) were then calculated for the optimized structures. The spin contamination resulting from the unrestricted formalism calculation of the radicals is small. The range of S^2 is from 0.759 to 0.765, with an average of 0.761.

Garrett and Serianni [20] have compared the energetic and geometric parameters calculated by ab initio optimization at the 3-21G and 6-31G* levels and observed semiquantitative agreement between the results from the two different basis set calculations. They concluded that the 3-21G basis set is sufficient for intact carbohydrates. In this study, we have computed the structures of two ribose minimum energy conformations and two ribose 2′-radical minimum energy conformations optimized at the 6-31G* level and compared them with those of the 6-31G results. Our comparison shows that in both ribose and its radicals the geometric and energetic parameters obtained by 6-31G and 6-31G* optimizations agree with each other quantitatively. Therefore, our systematic search and study of the minimum conformations of ribose and its radicals are conducted at the HF 6-31G level.

The puckering amplitude q_m and the pseudorotation phase angle ϕ of the furanose ring were calculated according to the definition of Cremer and Pople.[21] The pseudorotation parameter set (q_m,ϕ) are then converted to (τ_m,P) according to[22]

$$\tau_m(\text{deg}) = 102.5^\circ\, q_m\,(\text{Å})$$

$$P = \phi + 90^\circ$$

The puckering amplitude τ_m and the pseudorotation phase angle P calculated here are different from those defined by Altona and Sundaralingam,[23] but the actual numerical differences between the values calculated by these two methods are small.

The notation for the various pseudorotational conformations is as described previously.[10] "E" designates an envelope and "T" a twist conformation. The superscripts and subscripts designate respectively an *endo* (up) or an *exo* (down) state of the particular ring atom. For example, $^3T_4$ means a C_3-*endo*, C_4-*exo* twist conformation.

Results and Discussion

Minimum Energy Conformations of Ribose. Structural optimization yielded five minimum energy conformations of ribose. Four of them are shown in Figure 1. They can be classified into two N-type and two S-type structures. Within each group they can be distinguished by different 2-OH and 3-OH orientations. Selected structural parameters that distinguish the various isomers are listed in Table 1 together with the puckering amplitude τ_m and the pseudorotation phase angle P.

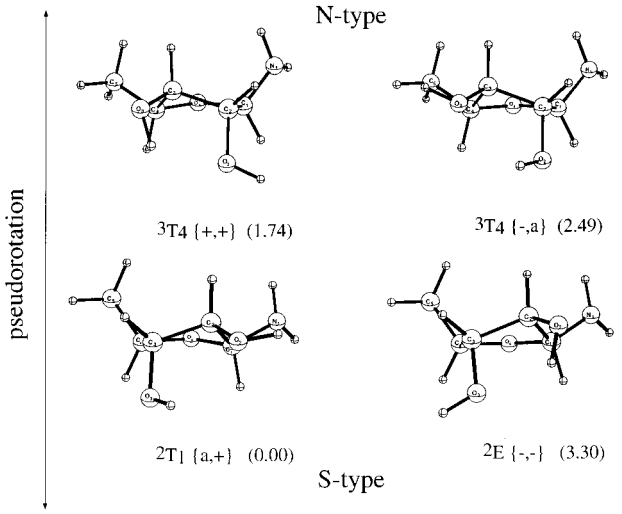

Figure 1. Four minimum energy structures of ribose: upper row, N-type; lower row: S-type. For detailed explanation, see text.

The symbol of each structure characterizes the pseudorotational state[10] and the orientations of the 3-OH and 2-OH groups, respectively. For example, in the N-type structure $^3T_4$ with $P = 27.6^\circ$ (close to the 3-*endo* conformer ^{3}E with $P = 18^\circ$) the dihedral angles of the hydroxyl groups ($H_{O3}O_3C_3C_4$ and $H_{O2}O_2C_2C_1$) are 81.8° and 76.4°, respectively. They are both in the +gauche region, hence the notation "{+,+}". The notations for the other conformers in Figure 1 and in Table 1 are defined similarly, where {−} signifies a −gauche, and {a} an anti conformation. The experimental values[24,23,10] are listed in parentheses for comparison. To assess the effect of the level of theory used in optimization, we have listed in Table 1, columns 2 and 6, the corresponding parameters from the two ribose minimum energy structures optimized at the HF/6-31G* level.

In all conformations the orientations of the OH groups is such that the hydrogen of one OH group is pointing to the oxygen of the other. In $^3T_4${+,+}, $_2E${+,−} and $^2T_1${a,+}, the distances between the hydrogen of the 3-OH group and the O_2 are 2.132, 2.211, and 2.213 Å, respectively. Similarly, in $^3T_4${−,a} and ^2E{−,−}, the distances between the hydrogen of the 2-OH group and the O_3 are 2.181 and 2.151 Å, respectively. While these distances are somewhat longer than standard hydrogen bonds, they suggest that the interaction between the two hydroxyl groups preferentially stabilizes these conformations through long-range hydrogen bonding or polar interactions. It is worth noting that the $_2E${+,−} structure is not a simple reorientation of the 2-OH group from a +gauche to a −gauche in the $^3T_4${+,+} structure. As can be seen from Table 1, this conformation, while belonging to the N-type, has a very different P of 342.1°, which may explain its relatively higher energy.

The energies of the HF/6-31G optimized structures, the zero-point energies (ZPE), dipole moments, and single-point energies at higher computational levels are listed in Table 2. The energies calculated for the two structures optimized at HF/6-31G* level are also listed in Table 2 (in parentheses). From both geometric and energetic aspects, the calculations at the HF/6-31G level give results that are quantitatively in agreement with those at the HF/6-31G* level. The puckering amplitude is slightly larger and the dipole moment is smaller for the HF/6-31G* optimized structures, but the ring dihedral angles and the orientations of the two OH groups are essentially the same. In the following discussion of ribose we will focus on the results from the HF/6-31G optimized structures only.

TABLE 1: Selected Structural Parameters of the Ribose Conformers[a]

	N-type				S-type		
	$^{3T}{}_4\{+,+\}$	$_4T^3\{+,+\}^\dagger$	$_2E\{+,-\}$	$^3T_4\{-,a\}$	$^2T_1\{a,+\}$	$^2T_1\{a,+\}^\dagger$	$^2E\{-,-\}$
pseudorotation parameters (deg)							
τ_m	37.2 (31−42)	39.2	39.8	38.9	39.9 (32−44)	41.1	37.3
P	27.6 (2−34)	41.2	342.1	26.9	150.8 (139−213)	149.3	159.3
endocyclic dihedral angles (deg)							
ν_0	−7.9 (3.2)	−18.5	24.5	−7.8	−31.1 (−23.5)	−33.6	−24.6
ν_1	−16.1 (−25.6)	−7.8	−37.8	−17.3	40.0 (36.9)	41.8	35.8
ν_2	32.6 (36.9)	28.4	37.5	34.4	−34.5 (−35.7)	−34.2	−34.6
ν_3	−36.8 (35.9)	−39.6	−22.9	−38.5	16.2 (22.9)	15.5	20.1
ν_4	28.5 (20.8)	37.1	−1.0	29.3	9.5 (0.2)	11.4	2.9
dihedral angles of OH (deg)							
$H_{O2}O_2C_2C_1$	76.4	75.3	−23.4	−157.6	55.9	49.9	−78.0
$H_{O3}O_3C_3C_4$	81.8	84.6	86.6	−76.1	157.2	156.2	−71.5

[a] All results are from the structures optimized at HF/6-31G level, except those two columns marked with † that are from the structures optimized at HF/6-31G* level.

TABLE 2: Energies and Dipole Moments of Ribose Conformers[a]

	N-type			S-type	
	$^3T_4\{+,+\}$	$_2E\{+,-\}$	$^3T_4\{-,a\}$	$^2T_1\{a,+\}$	$^2E\{-,-\}$
energies (hartree)					
HF/6-31G	−474.554251	−474.550739	−474.552692	−474.557570	−474.551414
HF/6-31G*	−474.748361 (−474.754591)	−474.744362	−474.745913	−474.751899 (−474.757803)	−474.744916
MP2/6-31G*	−476.129140 (−476.132805)	−476.127287	−476.126939	−476.133195 (−476.136806)	−476.126037
BLYP/6-31G*	−477.356646	−477.354526	−477.354333	−477.359836	−477.353822
BH/6-31G(d,p)	−477.301999	−477.299037	−477.299719	−477.305507	−477.299125
ZPE (kcal/mol)	115.61 (116.33)	115.46	115.38	115.95 (116.61)	115.39
energies relative to $^2T_1\{a,+\}$ (kcal/mol)					
HF/6-31G	2.08	4.29	3.06	0.00	3.86
HF/6-31G*	2.22 (2.01)	4.73	3.76	0.00	4.38
MP2/6-31G*	2.54 (2.51)	3.71	3.93	0.00	4.49
BLYP/6-31G*	2.00	3.33	3.45	0.00	3.77
BH/6-31G(d,p)	2.20	4.06	3.63	0.00	4.01
ZPE	−0.34 (−0.28)	−0.48	−0.57	0.00	−0.56
dipole moments (debye)					
μ_D	2.61 (1.85)	2.07	3.91	2.67 (1.93)	3.70

[a] All energy values are calculated on structures optimized at the HF/6-31G level, except those in parentheses which are from HF/6-31G* optimized structures.

The conformer $^2T_1\{a,+\}$ has the lowest energy at all the computational levels; thus it has been selected as the reference structure with respect to which the relative energies are calculated. Only minor reversals in the ordering of the different conformers occur as the level of computation changes. Among the four major conformers the ordering is $^2T_1\{a,+\} < {}^3T_4\{+,+\} < {}^3T_4\{-,a\} < {}^2E\{-,-\}$. It is interesting to note that the S-type conformation $^2T_1\{a,+\}$ is the most stable, in clear disagreement with the known preference of the ribose ring for the N-type conformation. However, an examination of this structure (see Figure 1) shows that the hydrogen of the 2-OH group is 2.899 Å from the N atom and the OH dipole is antiparallel to the C_1-N bond dipole. This probably contributes a significant portion of the stabilization of this conformer, because its ring conformation, characterized by τ_m and P, is very similar to that of the other S-type structure $^2E\{-,-\}$, in which the OH is not oriented toward the NH_2 group. The main difference between the two structures is the orientations of the 2-OH and 3-OH groups, but the 3.30 kcal/mol difference between these structure seems to include the loss of the $OH-NH_2$ interaction. In the N-type conformers, the structures of $^3T_4\{+,+\}$ and $^3T_4\{-,a\}$ show the same reorientation of the 3-OH and 2-OH groups with an increase in energy of 0.98 kcal/mol. Since this reorientation is not confounded by the $OH\cdots NH_2$ proximity, we can estimate the magnitude of this interaction to be approximately 2.32 kcal/mol. This allows us to estimate the pseudorotational energy difference between the N-type $^3T_4\{+,+\}$ and the S-type $^2T_1\{a,+\}$ around −0.68 (1.74−2.32) kcal/mol in favor of the N-type form. A similar analysis can be applied to the pseudorotational energy difference between $^3T_4\{-,a\}$and $^2E\{-,-\}$, which yields −0.81 kcal/mol. Thus we can conclude that the N-type conformers of ribose are more stable than the S-type by approximately 0.7 kcal/mol. As can be seen from Table 2, the dipole moments of the two corresponding N-type and S-type conformer pairs are similar. Thus, while the relative energies between the two N-type and the two S-type conformers may become more similar in an aqueous environment, the relative energies of the pseudorotamers will not depend on solvent.

It is interesting to consider the effect of the polyribonucleotide environment on the energetic preference of the N-type over the S-type conformers. Compilation of experimental data shows that in A-RNA, the dihedral angle ϵ ($C_4'-C_3'-O_3'-P$) is in the −antiperiplanar (−ap) region, with an average around 202°.[10] It is clear from Table 1 that the 3-OH in $^3T_4\{-,a\}$ and

TABLE 3: Structural Parameters of the C_1 Radicals of Ribose

	N-type		S-type	
	$_4T^3(+)$	$^3T_2(-)$	$^2E(+)$	$_3E(-)$
pseudorotation parameters (deg)				
τ_m	35.5	34.0	32.0	30.6
P	42.2	10.9	164.6	200.8
endocyclic dihedral angles (deg)				
ν_0	−17.0	4.4	−19.8	2.2
ν_1	−6.4	−23.6	31.3	16.6
ν_2	25.6	32.7	−30.3	−27.9
ν_3	−35.3	−30.5	19.6	29.5
ν_4	32.8	16.8	−0.4	−20.3
radical dihedral angles (deg)				
⊙ $C_1C_2O_2$	−0.8	−157.3	40.7	−113.8
⊙ $C_1C_2H_2$	123.0	−33.3	164.4	8.6
⊙ $C_1C_2C_3$	−114.0	90.1	−77.6	127.1
energies (hartree)				
HF/6-31G	−473.933632	−473.938048	−473.932719	−473.934406
BH/6-31G(d,p)	−476.649058	−476.653857	−476.648231	−476.651279
ZPE (kcal/mol)	106.23	106.98	106.45	106.87
relative energies (kcal/mol)				
HF/6-31G	2.77	0.00	3.34	2.29
ZPE	−0.75	0.00	−0.52	−0.11
dipole moments (debye)				
μ_D	2.86	3.20	3.15	1.85

$^2E\{-,-\}$ adopts the conformation −ac with values around 285°, which is close to the −ap region. It is likely that connecting the 3-OH group to phosphate in RNA will change the energy difference between $^2T_1\{a,+\}$ and $^2E\{-,-\}$ in the S-type pseudorotamers or between $^3T_4\{+,+\}$ and $^3T_4\{-,a\}$ in the N-type forms. However, the energy difference between the N-type and S-type conformers with the same 3-OH and 2-OH orientations is less likely to be changed by such environmental factors. Therefore, it is likely that the relative stability of N-type over S-type conformers of ribose in RNA is partly due to the pseudorotational energy difference similar to that between ribose conformations $^3T_4\{-,a\}$ and $^2E\{-,-\}$.

Minimum Energy Conformations of Ribose Radicals. To investigate the properties and conformations of ribose radicals we chose the N-type conformer $^3T_4\{+,+\}$ and S-type conformer $^2T_1\{a,+\}$ of ribose as representative conformations of the two pseudorotamer families. In this choice we have disregarded the dependence of the properties of these radical on the rotational orientation of the 2-OH and 3-OH groups. As discussed above, the relative energetics of the N-type versus the S-type conformers is largely independent of this orientation. Also, the conclusions regarding bond dissociation energy (BDE) of the various C−H bonds do not depend much on conformation (see below). Finally, we chose these conformations for the sake of comparison with our previous study of deoxyribose and its radicals,[5] in which the 3-OH group was oriented in a similar way. It is important to note that the radicals present an increased structural complexity because the radical center may invert its configuration, as we discuss in detail in the following.

1. C_1 Radicals. The optimized structures of N-type and S-type ribose C_1 radicals resulting from H-abstraction are shown in Figure 2. The symbols, such as $_4T^3$, denote the positions of the conformers on the polar pseudorotation map and the sign in parentheses indicates the orientation of the exocyclic NH_2 group at the radical center. A "+" means that the $-NH_2$ group is *endo* and a "−" designates an *exo* orientation. There are four stable structures which are local minima on the potential energy surface interconverting N-type to S-type conformers (vertical direction) or *endo* to *exo* radicals (horizontal direction).

The major geometric parameters, energies, and dipole moments of the four conformers in Figure 2 are listed in Table 3.

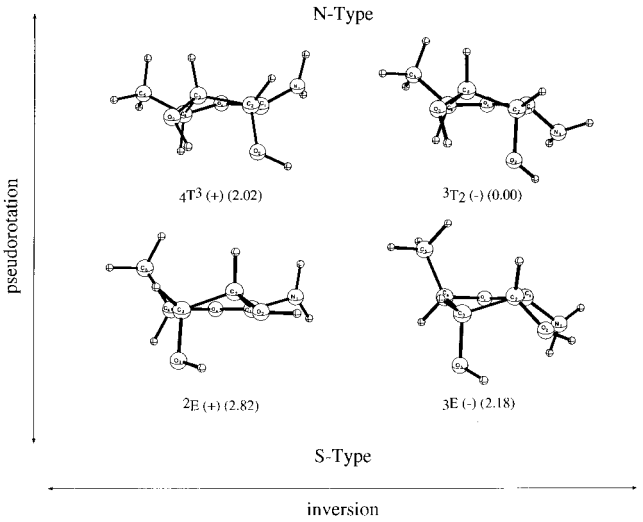

Figure 2. Ribose C_1 radical structures: upper row, N-type; lower row, S-type. Left column: uninverted conformations with NH_2 group in *endo* orientation. Right column: inverted conformations with NH_2 group in *exo* orientation.

To help in the discussion of the various energetic components that contribute to the relative stability of the N-type and S-type pseudorotamers and the two isomers related by inversion of the radical center, we have added three torsional angles of the "direction" of the unpaired electron with respect to the three substituents on C_2, namely O_2, H_2, and C_3. The "direction" of the unpaired electron is defined as the mean of the torsional angles $N_1C_1C_2O_2$ and $O_4C_1C_2O_2$. As can be seen from Table 3, in the structure $_4T^3(+)$ the unpaired electron (⊙) is eclipsed with the C_2O_2 bond and in $_3E(-)$ it is eclipsed with the C_2H_2 bond.

There are two isomerization axes in Figure 2. The vertical is the pseudorotation that interconverts between N-type and S-type isomers. Along the horizontal axis the radical center inverts from an *endo* (+) to an *exo* (−) orientation. As can be clearly seen from the relative energies of the isomers, the inversion process lowers the energies of the radicals that are formed by H abstraction from C_1. The ZPE-corrected energy difference between the (+) and the (−) conformers is 2.02 kcal/mol for the N-type radical, whereas for the S-type radical the energy

TABLE 4: Selected Structural Parameters and Energies of the C_2 Radicals of Ribose[a]

	$^0_4$T(−)	$_4$E(+)	$_4$E(+)†	^{2}T$_1$(−)	$_1$T^0(−)†	^{2}T$_3$(+)
pseudorotation parameters (deg)						
τ_m	33.0	29.8	33.3	26.8	31.4	32.2
P	70.1	55.2	55.3	148.7	120.5	167.8
endocyclic dihedral angles (deg)						
ν_0	−28.7	−20.0	−23.1	−21.6	−33.8	−16.8
ν_1	9.4	0.6	1.1	28.4	30.8	30.2
ν_2	11.0	17.2	18.6	−24.1	−16.4	−32.2
ν_3	−27.5	−28.2	−32.0	10.1	−3.7	21.2
ν_4	36.3	31.3	35.8	7.6	24.3	−2.7
radical dihedral angles (deg)						
⊙ $C_2C_3O_3$	119.3	26.9	27.8	−161.0	−151.6	−33.6
⊙ $C_2C_3H_3$	1.2	151.3	153.2	−37.7	−27.5	91.0
⊙ $C_2C_3C_4$	−120.2	−90.4	−90.5	84.0	92.3	−147.4
energies (hartree)						
HF/6-31G	−473.927821	−473.932918	−474.133182	−473.933334	−474.132914	−473.920687
BH/6-31G(d,p)	−476.644154	−476.649212		−476.647934		−476.635020
ZPE	106.28	106.67	107.4	106.87	107.5	106.44
relative energies (kcal/mol)						
HF/6-31G	3.46	0.26	−0.17	0.00	0.00	7.94
ZPE	−0.59	−0.20	0.10	0.00	0.00	−0.43
dipole moments (debye)						
μ_D	3.95	2.22	1.77	2.24	1.55	3.66

[a] All results are from the structures optimized at HF/6-31G level, except those two columns marked with † which are from the structures optimized at HF/6-31G* level.

difference is only 0.64 kcal/mol at the HF/6-31G level. This large energy difference between the radical inversion in the N-type vs the S-type can be attributed to the fact that in the N-type conformation the inversion to $^3T_2(-)$ forms an interaction between the 2-OH and the NH_2 groups, whereas in the S-type this interaction is present in both conformations. This is consistent with the differences in the ZPE-corrected barriers for the (+) → (−) transition. In the N-type, where an incipient 2-OH···NH_2 interaction is formed, the barrier is 0.52 kcal/mol whereas in the S-type the barrier is 1.50 kcal/mol because the interaction is present throughout the inversion.

The 2-OH···NH_2 interaction is also responsible for the large difference in the pseudorotation of the (+) radical, which is only 0.8 kcal/mol, compared to that of the (−) radical, which is 2.18 kcal/mol. Since the pseudorotation in the (−) radical does not form the 2-OH···NH_2 interaction, the 2.18 kcal/mol is a more likely energetic difference between the N-type and S-type pseudorotamers of the C_1 radical. Taking into account the formation of the 2-OH···NH_2 interaction in the (+) radical, the pseudorotation difference between the N-type and S-type radicals can be estimated around 2.8 kcal/mol. It is possible that the difference in the pseudorotation energy between the (+) and (−) radicals is due to different interactions of the unpaired electron with the adjacent bonds. Nevertheless, these results clearly indicate that the S-type conformation of the C_1 radical is less stable than the N-type by about 2.2−2.8 kcal/mol. The energy values calculated at other levels show the same qualitative features.

The inversion at the radical center may have interesting implication to conformational rearrangement in oligoribonucleotides upon H abstraction. The relatively low barrier and the preferred stability of the (−) form could induce an inversion of the C_1' radical. Since the base is constrained by Watson−Crick hydrogen bonds and by stacking interactions with adjacent bases, the ring may alter its orientation, transmitting the change at the radical center to the backbone conformation.

2. C_2 Radicals. The radicals produced by abstracting H_2 of ribose are shown in Figure 3. Their structural parameters, energies and dipole moments are listed in Table 4. Two columns, marked by †, that list results from the corresponding HF/6-31G* optimized structures, are included in Table 4 for comparison. Similar to ribose, a slightly larger puckering amplitude, a much smaller dipole moment, and quantitatively similar results for dihedral angles and energies are found for C_2 radicals. The comparison between optimization levels at HF/6-31G* with that at HF/6-31G shows that also in the radicals, HF/6-31G optimization produces essentially the same structures as those by HF/6-31G* optimization. In the following our discussion will involve HF/6-31G optimized structures only.

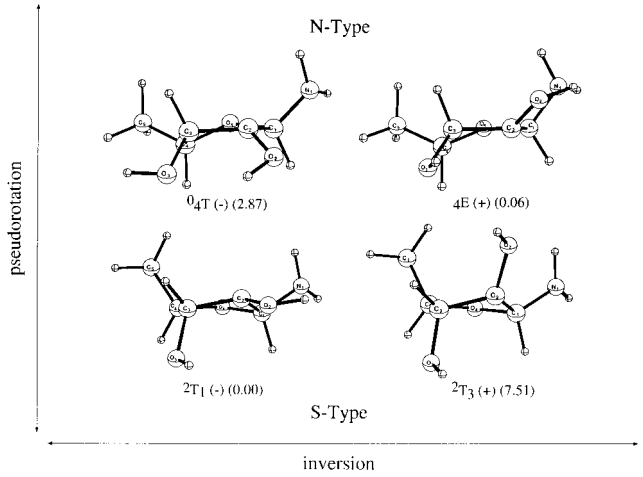

Figure 3. Ribose C_2 radical structures: upper row, N-type; lower row, S-type. Left column: uninverted conformations with 2-OH group in *exo* orientation. Right column: inverted conformations with NH_2 group in *endo* orientation.

The abstraction of H_2 from the N-type conformation of ribose produces the $^0_4$T(−) form with the 2-OH group in an *exo* orientation. The energy of this conformer is 2.81 kcal/mol higher than the $_4$E(+) form, in which the 2-OH is inverted into the *endo* orientation. It appears that the inversion is stabilized by the OH···NH_2 interaction as can be seen from the proximity of the 2-OH group to the amine. An alternative way of stabilizing the $^0_4$T(−) conformer is by pseudorotation to the S-type form. The ^{2}T$_1$(−) form is 2.87 kcal/mol more stable and here also the stabilization is probably produced by the OH···NH_2 interaction. The inversion of the ^{2}T$_1$(−) to the ^{2}E(+) is highly unlikely

TABLE 5: Selected Structural Parameters and Energies of the C_3 Radicals of Ribose

	N-type		S-type	
	$^3T_2(-)$	$_2E(+)$	$_1T^0(-)$	$^2{}_1T(+)$
pseudorotation parameters (deg)				
τ_m	26.5	34.7	34.4	34.7
P	11.4	340.6	115.9	144.4
endocyclic dihedral angles (deg)				
ν_0	2.5	22.4	−37.1	−30.1
ν_1	−17.7	−33.1	30.4	34.5
ν_2	27.0	33.1	−15.0	−29.0
ν_3	−25.2	−20.2	−6.2	11.6
ν_4	13.6	−1.8	27.3	12.1
radical dihedral angles (deg)				
⊙ $C_3C_4O_4$	68.6	−133.2	104.0	−94.8
⊙ $C_3C_4H_4$	−158.5	−20.3	−140.2	20.7
⊙ $C_3C_4C_5$	−32.9	105.9	−14.5	146.8
energies (hartree)				
HF/6-31G	−473.927489	−473.921225	−473.932607	−473.931299
BH/6-31G(d,p)	−476.640676	−476.635645	−476.648156	−476.646607
ZPE	106.30	106.41	106.68	106.57
relative energies (kcal/mol)				
HF/6-31G	3.21	7.14	0.00	0.82
ZPE	−0.38	−0.27	0.00	−0.11
dipole moments (debye)				
μ_D	3.54	2.40	2.86	2.40

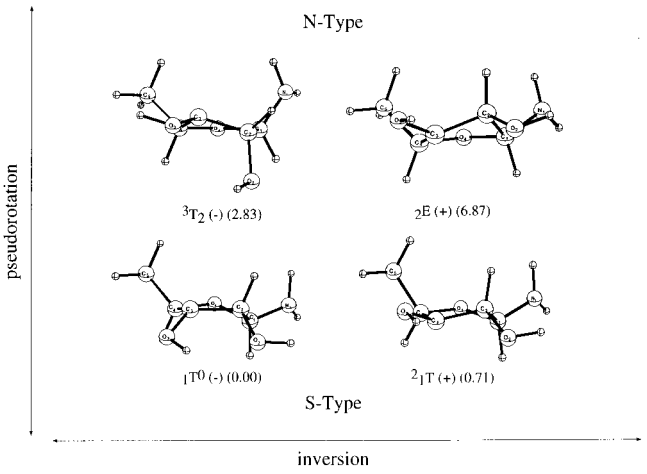

Figure 4. Ribose C_3 radical structures: upper row, N-type; lower row, S-type. Left column: uninverted conformations with 3-OH group in *exo* orientation. Right column: inverted conformations with NH_2 group in *endo* orientation.

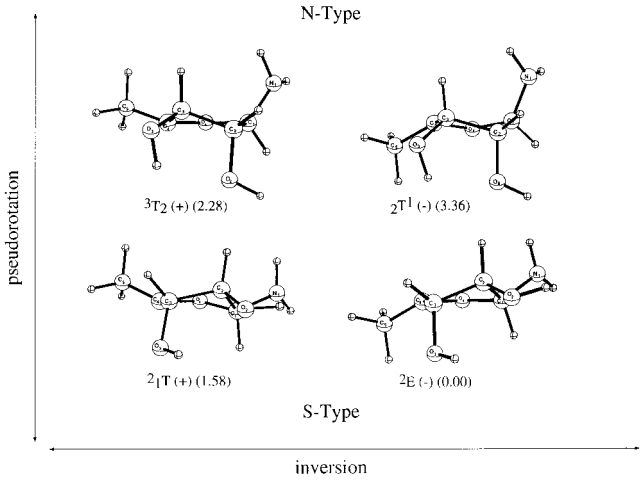

Figure 5. Ribose C_4 radical structures: upper row, N-type; lower row, S-type. Left column: uninverted conformations with 5-CH_3 group in *endo* orientation. Right column: inverted conformations with NH_2 group in *exo* orientation.

because the energy of the $^2E(+)$ form is 7.50 kcal/mol higher than that of the other S-type conformer. An additional factor that may contribute to the instability of the N-type $^0{}_4T(-)$ conformation is the repulsion between the unpaired electron on C_2 and the N atom, which almost eclipse each other.

The energy difference between the N-type and S-type, ΔE_{N-S}, in the C_2 radicals is very small (0.06 kcal/mol) at the HF/6-31G level. The flatness of the ring, as indicated by the small values of τ_m, may be the reason that the interconversion between the N-type and S-type conformers of C_2 radical couples inversion to pseudorotation. This leads to an apparent lack of preference for a specific pseudorotamer in the C_2 radicals.

3. C_3 Radicals. The radicals produced by abstraction of H_3 from ribose are shown in Figure 4 and selected structural parameters and energies are shown in Table 5. The abstraction of H_3 from the N-type ribose yields the $^3T_2(-)$ form of the C_3 radical. The inverted form of N-type C_3 radical, $_2E(+)$, is much higher in energy and is therefore unlikely to be formed by inversion. On the other hand, the S-type radical, $_1T^0(-)$ that can be formed from $^3T_2(-)$ by pseudorotation is lower in energy by 2.84 kcal/mol. Part of this stabilization may originate from the 2-OH···NH_2 interaction, which forms as a consequence of pseudorotation. The $_1T^0(-)$ radical produced by inversion of the $^2{}_1T(+)$ radical is only 0.72 kcal/mol higher in energy and is easily accessible. These data suggest that the S-type C_3 radicals are more stable than the N-type. Even if we take into consideration the stabilization due to the 2-OH···NH_2 interaction, which should not exceed 2 kcal/mol, this conclusion should hold. Thus, introduction of a radical on C_3 in oligoribonucleotides and RNA may lead to a change in the preferred pseudorotational state from the N-type to the S-type. The small energetic difference between the *exo* (−) and the *endo* (+) conformers of the S-type radical suggests that the inversion could couple to the pseudorotation and play an important role in stabilizing the distorted backbone of RNA containing a C_3 radical. This large value of ΔE_{N-S} is also maintained at other levels of computation.

4. C_4 Radicals. The N-type and S-type radicals that result from abstracting H_4 of ribose are shown in Figure 5. Selected structural parameters and energies are shown in Table 6. The N-type C_4 radical, $^3T_2(+)$, is more stable than the inverted radical $_2T^1(-)$ by 0.49 kcal/mol. The inversion of the $^3T_2(+)$

TABLE 6: Selected Structural Parameters and Energies of the C_4 Radicals of Ribose

	N-type		S-type	
	$^3T_2(+)$	$_2T^1(-)$	$^2{}_1T(+)$	$^2E(-)$
pseudorotation parameters (deg)				
τ_m	31.8	32.2	38.4	37.3
P	5.9	329.4	145.5	164.7
endocyclic dihedral angles (deg)				
ν_0	6.1	25.8	−32.0	−21.1
ν_1	−23.3	−32.2	38.4	34.8
ν_2	31.0	27.0	−30.9	−35.4
ν_3	−28.2	−12.3	12.1	23.5
ν_4	14.3	−8.6	12.8	−1.6
radical dihedral angles (deg)				
⊙ $C_4C_3C_2$	80.2	−119.6	−62.9	−84.1
⊙ $C_4C_3H_3$	−162.3	−1.6	58.1	37.4
⊙ $C_4C_3O_3$	−42.9	117.5	−179.6	159.9
energies (hartree)				
HF/6-31G	−473.932046	−473.931336	−473.934239	−473.937198
BH/6-31G(d,p)	−476.647524	−476.646293	−476.650902	−476.652602
ZPE	106.34	106.39	106.43	106.71
relative energies (kcal/mol)				
HF/6-31G	2.65	3.68	1.86	0.00
ZPE	−0.37	−0.32	−0.28	0.00
dipole moment (debye)				
μ_D	2.96	3.01	3.36	2.88

radical is unfavorable because of the eclipsing of the CH_3 group with the 3-OH in the inverted form $_2T^1(-)$. On the other hand, the S-type radical $^2{}_1T(+)$ can reduce its energy by inverting the CH_3 group at the radical center from an *endo* to an *exo* orientation. The resulting conformer, $^2E(-)$, is stabilized by 1.58 kcal/mol, which can be attributed to relieving the repulsion between the unpaired electron and the lone pair on O_3 in the $^2{}_1T(+)$ radical. The pseudorotation from the N-type to the S-type forms is also favorable, but it stabilizes the S-form radical $^2{}_1T(+)$ by 1.29 kcal/mol in spite of the formation of a 2-OH···NH_2 interaction. This would suggest that pseudorotation alone would not stabilize the S form in favor of the N form of the C_4 ribose radical. However, when the pseudorotation is coupled to an inversion resulting in the $^2E(-)$ form, the S-type radical may be more stable than the N-type form. Thus, introduction of a C_4 radical into oligoribonucleotides should generate a distortion expressed as a S-type sugar pseudorotation an inverted center around C_4.

General Geometric Features of the Radicals. All the carbon-centered radicals of ribose share some common features of geometric changes with respect to ribose. Radical formation is usually accompanied by a hyperconjugation with neighboring groups as noticed in the rehybridization of the sp^3 orbital of the unpaired electron to appear more like an sp^2. The hyperconjugation increases the angles around the radical by 4°−7° and shortens the bond lengths between the radical center and its neighboring atoms. Because the radical center is in a ring, the other endocyclic bond lengths and bond angles adjust to accommodate these changes. In general, the endocyclic bond angles on the two neighboring ring atoms tend to decrease and the two other endocyclic bond lengths tend to increase. These common features are similar to those found in deoxyribose radicals.[5]

The rehybridization, which leads to a flattening of the radical center, can be best illustrated by the changes in improper dihedral angles. For example, the improper dihedral angle, ϕ_{imp}, around C_1 ($O_4C_1N_1C_2$) is defined as the angle between the plane $O_4C_1N_1$ and the plane $C_1N_1C_2$. The amplitude of ϕ_{imp} of a perfect tetrahedral center is 120°, while that of a planar center is 180°. The improper dihedral angles of the other three radical centers are defined in a similar way such that they are positive for an *endo* and negative for an *exo* heavy branch group. The improper angles of ribose and of the radicals are listed in Table 7. The improper dihedrals of ribose average around 115° with the C_1 and C_4 being positive and those at C_2 and C_3 negative. The absolute values of the ϕ_{imp} at the radical centers show significant increases, on the average about 25°, confirming that the radical centers are flattening. One important difference between the C_2 radical of ribose and of deoxyribose[5] is that the ribose C_2 radical is not significantly different from the other radicals, whereas the C_2 radical of deoxyribose was much more flat than all the others. As before,[5] the mechanism of the lesser flattening of the radical on C_2 in ribose is because it is positioned α to an oxygen (O_2). Since the same is true for the other ring carbons, the distinction of the C_2 radical in deoxyribose is lost in the C_2 radical in ribose.

TABLE 7: Average Improper Dihedral Angles and Puckering Amplitudes

	ϕ_{imp}	τ_m
ribose	115.8 ± 1.3	38.3 ± 1.3
radicals		
C_1	136.5 ± 4.7	33.0 ± 2.2
C_2	136.5 ± 6.9	30.5 ± 2.8
C_3	135.5 ± 5.7	32.6 ± 4.0
C_4	143.6 ± 3.4	34.9 ± 3.4

The flattening of the ring, as characterized by the decrease in puckering amplitude τ_m shown in Table 7, is another general property of ribose radicals. Clearly, the decrease from 38.3° for ribose to values between 28° and 35.8° indicates that the ring becomes more flat upon radical formation. However, the flattening around the radical center and flattening of the ring do not show a simple relationship, suggesting that they are conceptually different and represent different properties of the ring. Ribose ring puckers in the first place to stagger the exocyclic branch groups in order to reduce the steric conflict between adjacent groups. Flattening around the radical center changes the orientation of the remaining branch groups connected to the radical center and makes the staggering of adjacent substituents unnecessary. This in turn leads to a reduction in the amplitudes of the two endocyclic dihedral angles centered at the radical carbon. When the two dihedral angles have a large amplitude, the resulting decrease in the puckering amplitude τ_m is large. For example, the endocyclic dihedral angles ν_1 and

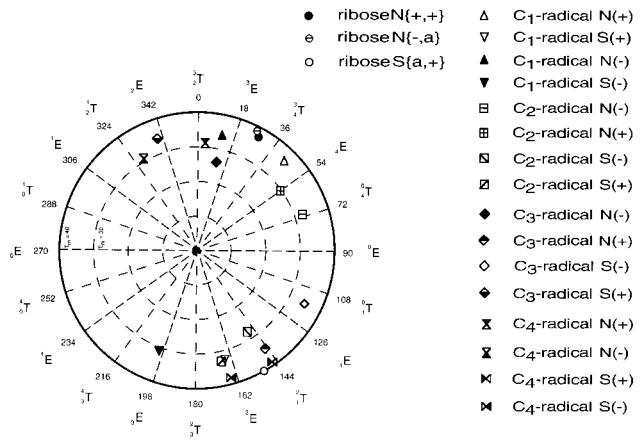

Figure 6. Ribose and its radicals on (τ_m, *P*) pseudorotation map.

ν_2 in S-type ribose conformation $^2T_1\{a,+\}$ are 40.0° and −34.5°, respectively. The formation of the S-type C_2 radical, with a radical center positioned between ν_1 and ν_2, leads to the greatest reduction in τ_m, from 39.9° to 26.8°. Similarly, the endocyclic dihedral angles ν_3 and ν_2 in N-type ribose conformation $^3T_4\{-,a\}$ are −38.5° and 34.4°, respectively. Again, the reduction in τ_m from 38.9° to 26.5° occurs in N-type C_3 radical $^3T_2(-)$, in which the radical is formed between the two endocyclic dihedrals. A similar behavior was observed in deoxyribose radicals, where the S-type ring conformation is most flattened in the C_2 radical and the N-type in the C_3 radical.[5] In general, the inversion of those radical centers that reduces energy tends to further decrease in τ_m, as expected, since the inversion further reduces the steric conflict between the adjacent branch groups.

Shift of Pseudorotational Phase Angle *P* in Ribose Radicals Relative to Ribose. The (τ_m, *P*) values of three ribose minimum energy conformations and four minimum energy conformations from each of the radicals are plotted on the polar coordinate map[10] in Figure 6. The position of each symbol shows its (τ_m, *P*) value, while the other degrees of freedom, including the orientations of the 2-OH and 3-OH groups in ribose, and the orientation of the branch group at the radical center for ribose radicals, are characterized by different symbols. The general pattern of the shift in pseudorotational angle *P* follows that of the deoxyribose radicals:[5] The C_1 and C_2 radicals shift clockwise relative to the ribose positions of both N- and S-types, while the C_3 and C_4 radicals shift counterclockwise. The underlying mechanism for the shift is the same as described for the deoxyribose case,[5] namely, the dihedral angles around the two endocyclic bonds centered at the radical tend to decrease in amplitude due to the reduced steric conflict, which induces a change in *P* in the described direction. As in deoxyribose, we also note that the changes in the endocyclic dihedral angles ν_0 of N-type C_1 radical $_4T^3(+)$ and ν_4 of S-type C_4 radical $^2{}_1T(+)$ do not decrease but rather increase in amplitude. This change reduces the interaction between the unpaired radical electron on C_1 or C_4 and the lone pair of O_4 when either ν_0 or ν_4 is close to zero in ribose. The exception of the S-type C_2 radical that is shifted counterclockwise is small (−2.1°) and can be understood in terms of *P*-shift dependence on the location of the maximum amplitude of ν_2 relative to the energy minima as was noted previously.[5]

In two inverted radicals, C_1 N(−) and C_4 S(−), the P-shift is opposite to the corresponding normal radicals. This is produced by eclipsing the nitrogen on C_1 with O_2 due to the inversion of the radical. To relieve the steric conflict, the amplitude of ν_1 increases to −23.6°, decreasing *P* to 10.9°. A similar situation occurs for the inverted S-type 4-radical, in which the conflict between O_3 and inverted C_5 increases ν_3 from 12.1° to 23.5°.

TABLE 8: Bond Dissociation Energy (in kcal/mol) of Hydrogens on the Ribose Ring

	HF/ 6-31G	HF/ 6-31G*	MP2/ 6-31G*	BLYP/ 6-31G*	BH/ 6-31G(d,p)
H_1	66.3	67.3	81.7	82.7	87.2
H_2	69.4	69.1	85.4	84.9	89.9
H_3	71.6	71.6	88.6	88.2	92.7
H_4	68.8	69.2	85.0	85.6	90.1

Energetics of Hydrogen Abstraction from Ribose. The dissociation energies (BDE) of the C−H bonds in ribose can be calculated from our results and they are listed in Table 8. These values are the Boltzmann averaged enthalpies at 298.15 K, calculated using the method of Pople et al.[25] Our previous study on the hydrogen abstraction from 2-propanol[26] shows that the scaling for the electron correlation is not completely uniform for carbons with different substituents. Therefore, we did not use the scaling proposed by Gordon and Truhlar[27] to estimate the electron correlation. Instead, we use density functional theory calculations with a larger basis set, BH/6-31G(d,p), to include the electron correlation in the BDE calculation. The differences between the BDE calculated at the HF/6-31G and HF/6-31G* levels are small, in most cases less than 1 kcal/mol, indicating that inclusion of polarization on heavy atoms does not have a significant effect on BDE of the C−H bonds of ribose at the uncorrelated level. The BDE values calculated at the MP2/6-31G* and BLYP/6-31G* levels are much larger and closer to each other, with differences between them of less than 3 kcal/mol. The inclusion of electron correlation significantly increases the BDE for all the C−H bonds by about 20%. However, their underestimation of correlation energy is apparent when compared with the BDE values calculated at the BH/6-31G(d,p) level. We take these values as the best available so far and we use them as the basis for the following discussion.

The BDE does not change very much for different conformers of the same radical, which led us to calculate the BDE as the Boltzmann average. The lowest BDE is for C_1−H bond and the highest for the C_3−H bond. In contrast to deoxyribose, the H_2 abstraction from ribose is not significantly different energetically from the abstraction of other ring hydrogens. Thus, these results confirm the conjecture that the presence of O_2 facilitates H abstraction from C_2.

Comparison with Deoxyribose and Its Radicals. The inversion of ring carbon radical centers also occurs in deoxyribose radicals (Luo, N.; Osman, R., unpublished data). Here we only summarize the parallel comparisons of the ribose and its radicals with deoxyribose and its radicals described in the previous study.[5]

Our studies show that in ribose the N-type conformation is more stable than the S-type, whereas the opposite was observed in deoxyribose. This is consistent with the common knowledge that deoxyribose is stable as the C_3'-*endo* conformation whereas the ribose is more stable as the C_2'-*endo*. The C_1 radical of ribose retains the energetic preference of the parent sugar, whereas in deoxyribose there is virtually no energetic preference of the N-type over the S-type conformer. The C_2 radical of ribose shows a similar energetic degeneracy as the C_1 radical of deoxyribose, but the C_2 radical of deoxyribose shows a distinct preference for the N-type conformer, which is different than the parent sugar. The C_3 radicals both show a preference for the S-type conformation indicating that the ribose has changed its preference with respect to the parent molecule. Both C_4 radicals change their preference compared to the parent sugars.

Overall, this behavior of the radicals leads to different effects in the oligonucleotide states. Whereas in DNA the major conformational changes will be forced by the C_2 and C_4 radicals, in RNA the major changes will come from C_3 and C_4 radicals. Since the formation of the C_4 radicals has been shown to be the most probable event in H abstraction from nucleic acids, the structural consequences are similar in both DNA and RNA.

For 2-, 3-, and 4-radicals, the N−S energy differences of ribose and deoxyribose have the same signs: negative for 2-radicals and positive for 3- and 4-radicals. The difference in the ribose 3 radicals is much larger, accompanied by the instability of the 2-OH +gauche orientation that all other minimum energy radical conformers take.

H_1 abstraction in both ribose and deoxyribose has the lowest enthalpy. H_2 abstraction in deoxyribose has the highest enthalpy, about 4 kcal/cal higher than H_3 and H_4 abstractions, but in ribose it is essentially the same as H_4, while H_3 abstraction becomes the highest (about 3 kcal/mol higher). Thus, the preference of H abstraction in both sugars is also similar, in view of the preferred abstraction of H_4.

The change in the puckering amplitude τ_m upon H abstraction exhibits a similar pattern in ribose as in deoxyribose as does the shifting of the pseudorotation phase angle P. In C_1 and C_2 radicals, the P values for both N- and S-types shift clockwise from the respective positions of their parent sugars on the (τ_m, P) dial (i.e., increasing P), while the C_3 and C_4 radicals shift counterclockwise (decreasing P).

Conclusions

In this study we have investigated the minimum energy conformations of ribose and the ribose radicals obtained by abstracting a hydrogen from one of the four ring carbons. We have shown the effects of the 2-OH group on the structure and energy of ribose and its radicals by comparing the results with those obtained for deoxyribose and its radicals. We have found that a wide range of structural and energetic characteristics run parallel in ribose and its radicals to those in the deoxyribose case. General geometry changes such as endocyclic bond lengths, bond angles, and dihedral angles, as well as the pseudorotational phase angle shift and puckering amplitude decrease upon H abstraction, follow a similar pattern in both sugars. These effects are, therefore, not very sensitive to the presence of the 2-OH group. However, there is an important difference between the bond dissociation energy of hydrogen abstraction from ribose and from deoxyribose: The BDE of H abstraction from C_2 of deoxyribose is significantly higher than that from other carbons, while in ribose this is not the case, demonstrating the effect of an α-oxygen in weakening the C−H bond. We have also found that the radical center inversion leads to lower energy in C_1 and C_4 radicals.

Acknowledgment. This work was supported by PHS grant CA-63317.

References and Notes

(1) von Sonntag, C. *The Chemical Basis of Radiation Biology*; Taylor & Francis: London, 1987.

(2) Hildenbrand, K.; Schulte-Frohlinde, D. *Int. J. Radiat. Biol.* **1989**, *55*, 725−738.

(3) Hildenbrand, K.; Schulte Frohlinde, D. *Free Radical Res. Commun.* **1990**, *11*, 195−206.

(4) Schulte-Frohlinde, D.; Simic, M. G.; Gorner, H. *Photochem. Photobiol.* **1990**, *52*, 1137−51.

(5) Miaskiewicz, K.; Osman, R. *J. Am. Chem. Soc.* **1994**, *116*, 232−8.

(6) Levitt, M.; Warshel, A. *J. Am. Chem. Soc.* **1978**, *100*, 2607−13.

(7) Saran, A.; Perahia, D.; Pullman, B. *Theor. Chim. Acta* **1973**, *30*, 31−44.

(8) Hole, E. O.; Nelson, W. H.; Sagstuen, E.; Close, D. M. *Radiat. Res.* **1992**, *130*, 148−159.

(9) Nelson, W. H.; Sagstuen, E.; Hole, E. O.; Close, D. M. *Radiat Res* **1992**, *131*, 272−284.

(10) Saenger, W. *Principles of Nucleic Acid Stucture*; Springer-Verlag: New York, 1984.

(11) van Wijk, J.; Huckriede, B. D.; Ippel, J. H.; Altona, C. *Methods Enzymol.* **1992**, *211*, 286−306.

(12) Weisz, K.; Shafer, R. H.; Egan, W.; James, T. L. *Biochemistry* **1994**, *33*, 354−66.

(13) Miura, T.; Thomas, G. J., Jr. *Biochemistry* **1994**, *33*, 7848−56.

(14) Liquier, J.; Taillandier, E.; Klinck, R.; Guittet, E.; Gouyette, C.; Huynh Dinh, T. *Nucl. Acids Res.* **1995**, *23*, 1722−8.

(15) Duker, J. M.; Serianni, A. S. *Carbohydr. Res.* **1993**, *249*, 281−303.

(16) Dalluge, J. J.; Hashizume, T.; Sopchik, A. E.; McCloskey, J. A.; Davis, D. R. *Nucl. Acids Res.* **1996**, *24*, 1073−9.

(17) Dagneaux, C.; Liquier, J.; Taillandier, E. *Biochemistry* **1995**, *34*, 16618−23.

(18) Colson, A.-O.; Sevilla, M. D. *J. Phys. Chem.* **1995**, *99*, 3867−74.

(19) Frisch, M. J.; Trucks, G. W.; Schlegel, H. B.; Gill, P. M. W.; Johnson, B. G.; Robb, M. A.; Cheeseman, J. R.; Keith, T. A.; Petersson, G. A.; Montgomery, J. A.; Raghavachari, K.; Al-Laham, M. A.; Zakrzewski, V. G.; Ortiz, J. V.; Foresman, J. B.; Cioslowski, J.; Stefanov, B. B.; Nanayakkara, A.; Challacombe, M.; Peng, C. Y.; Ayala, P. Y.; Chen, W.; Wong, M. W.; Andres, J. L.; Replogle, E. S.; Gomperts, R.; Martin, R. L.; Fox, D. J.; Binkley, J. S.; Defrees, D. J.; Baker, J.; Stewart, J. P.; Head-Gordon, M.; Gonzalez, C.; Pople, J. A. *Gaussian 94*, Revision B.3; Gaussian Inc.: Pittsburgh, PA, 1995.

(20) Garrett, E. C.; Serianni, A. S. *Carbohydr. Res.* **1990**, *206*, 183−191.

(21) Cremer, D.; Pople, J. A. *J. Am. Chem. Soc.* **1975**, *97*, 1354−8.

(22) Rao, S. T.; Westhof, E.; Sundaralingam, M. *Acta Crystallogr., Sect. A* **1981**, *A37*, 421−5.

(23) Altona, C.; Sundaralingam, M. *J. Am. Chem. Soc.* **1972**, *94*, 8205−12.

(24) Arnott, S.; Hukins, D. W. *Biochem. J.* **1972**, *130*, 453−465.

(25) Pople, J. A.; Luke, B. T.; Frisch, M. J. *J. Phys. Chem.* **1985**, *89*, 2198−203.

(26) Luo, N.; Kombo, D. C.; Osman, R. *J. Phys. Chem.* **1997**, *101*, 1 A, 926−936.

(27) Gordon, M. S.; Truhlar, D. G. *J. Am. Chem. Soc.* **1986**, *108*, 5412−5419.